ROBUSTNESS OF TIME REVERSAL FOR WAVES IN TIME-DEPENDENT RANDOM MEDIA

DANIEL G. ALFARO VIGO*, JEAN-PIERRE FOUQUE†, JOSSELIN GARNIER‡, AND ANDRÉ NACHBIN*

Abstract. This paper addresses the impact of time fluctuations of a random medium on refocusing during a time-reversal experiment. Even in the presence of moderate time-perturbations a coherent refocused pulse is observed. The theory predicts the level of recompression observed as well as the conditions for the loss of statistical stabilization. It is shown that the statistical properties of the refocused pulse depend on a simple set of parameters that describe the correlation degree of the medium. The refocused pulse has in general a random shape that can be described in terms of a system of stochastic transport equations driven by a single Brownian motion. Pulse stabilization is also demonstrated for some particular configurations, and the convolution kernel that describes the pulse reshaping is explicitly computed. Numerical simulations are presented and show a very good agreement with the theoretical predictions, thus providing a clear illustration of the robustness of time reversal.

Key words. Inhomogeneous media, asymptotic theory, time reversal.

AMS subject classifications. 35L05, 60H15, 74J20.

1. Introduction. In this paper we analyze the effect of a time dependent random medium on the time-reversed refocusing phenomenon. We consider linear acoustic waves propagating in a disordered one-dimensional medium. We demonstrate that even in the presence of moderate time-perturbations a coherent refocused pulse is observed. The theory also predicts the level of recompression observed as well as the conditions for the loss of statistical stabilization.

Time-reversal refocusing for waves propagating in inhomogeneous media have been recently observed and studied experimentally in various contexts, e.g. ultrasound, underwater acoustics, see for instance the review [11]. Important potential applications have been proposed in various fields, for instance imaging [20, 12] and communication [10]. A time-reversal mirror is, roughly speaking, a device which is capable of receiving a signal in time, keeping it in memory and sending it back into the medium in the reversed direction of time. The main effect is the refocusing of the scattered signal after time-reversal in a random medium. Surprisingly, the refocused pulse shape only depends on the statistical properties of the random medium, and not on the particular realization of the medium. The full mathematical understanding, meaning both modeling of the physical problem and derivation of the time-reversal effect, is a complex problem. The study of the one-dimensional linear case is now well understood [9, 21, 13] as well as the three-dimensional waves in the parabolic or paraxial regime [4, 6, 19]. In this paper we consider the situation where the medium changes from the forward experiment to the time-reversed experiment. This characterizes a time-dependent medium. Experimental results on the robustness of acoustic

*Instituto de Matemática Pura e Aplicada, Est. D. Castorina 110, Jardim Botânico, Rio de Janeiro, RJ 22460-320, Brazil. E-mails: dgalfaro@impa.br and nachbin@impa.br. URL: http://www.impa.br/~nachbin.

†Department of Mathematics, North Carolina State University, Raleigh NC 27695-8205. E-mail: fouque@math.ncsu.edu. URL: http://www.math.nscu.edu/~fouque.

‡Laboratoire de Statistique et Probabilités, Université Paul Sabatier, 118 Route de Narbonne, 31062 Toulouse Cedex 4, France. E-mail: garnier@cict.fr URL: http://www.lsp.ups-tlse.fr/Garnier

time-reversal refocusing in a multiple scattering medium undergoing perturbations are presented in [23]. Here we address theoretically and numerically for the first time the impact of such a time-fluctuating medium on the statistical properties of the pulse refocusing.

The paper is organized as follows. In Sections 2-6 we derive integral representations of the refocused pulse shapes in terms of reflection and transmission coefficients for the wave modes. Section 7, resp. 8, is devoted to the thorough analysis of time-reversal experiments in reflection, resp. in transmission. Section 9 presents results from full numerical simulations.

2. The acoustic model. We consider the acoustic wave equation

$$\frac{1}{K}\frac{\partial p}{\partial t} + \frac{\partial u}{\partial z} = 0 \tag{2.1}$$

$$\rho\frac{\partial u}{\partial t} + \frac{\partial p}{\partial z} = 0 \tag{2.2}$$

where p is the pressure and u is the velocity, z and t are the space and time coordinates, respectively. ρ is the density of the medium and K the bulk modulus. The medium is described by:

$$\rho \equiv \begin{cases} 1+\nu(\dfrac{z}{\varepsilon^2}) & \text{if } -L < z < 0 \\ 1 & \text{if } z > 0 \text{ and } z < -L \end{cases} \tag{2.3}$$

$$\frac{1}{K} = \begin{cases} 1+\eta(\dfrac{z}{\varepsilon^2}) & \text{if } -L < z < 0 \\ 1 & \text{if } z > 0 \text{ and } z < -L \end{cases} \tag{2.4}$$

where (η,ν) is a $\mathbb{R}^2$-valued mixing process. The dimensionless small parameter ε^2 characterizes the ratio of the correlation radius of the fluctuations of the medium and the typical size of the medium. These fluctuations are modeled by the zero-mean stationary random process $(\eta,\nu)(z)$. The processes η and ν are assumed to be bounded by a deterministic constant less than 1 and to have strong ergodic properties. We may think for instance that (η,ν) is a function of a Markov, stationary, ergodic process on a compact space satisfying the Fredholm alternative [18]. We can also work with the class of the ϕ-mixing processes with $\phi \in L^{1/2}$ [14].

We consider the problem on the finite slab $-L \le z \le 0$ where boundary conditions will be imposed at $-L$ and 0 corresponding to a pulse entering the slab from the right at $z = 0$. The quantities of interest, the transmitted and reflected waves, will be observed in time at the extremities $z = -L$ and $z = 0$, respectively.

We shall consider a pulse whose typical wavelength is of order ε, that is to say small compared to the size of the medium, but large with respect to the correlation length of the random medium:

$$f^\varepsilon(t) = f(\frac{t}{\varepsilon})$$

3. Propagator formulation. In this section we first express the scattering problem as a two point boundary value problem in the frequency domain, and then rewrite it as an initial value problem in terms of the propagator. This study follows the lines of the analysis carried out in Ref. [3].

FIG. 3.1. *Scattering problem.*

3.1. Mode propagation in the frequency domain. We consider the random acoustic equation (2.1-2.2) and take the scaled time Fourier transform

$$\hat{u}^\varepsilon(\omega,z)=\frac{1}{2\pi\varepsilon}\int u(t,z)\exp(-\frac{i\omega t}{\varepsilon})dt,\qquad \hat{p}^\varepsilon(\omega,z)=\frac{1}{2\pi\varepsilon}\int p(t,z)\exp(-\frac{i\omega t}{\varepsilon})dt$$

so that the system reduces to a set of ordinary differential equations:

$$\frac{\partial\hat{p}^\varepsilon}{\partial z}+\frac{i\omega}{\varepsilon}\left(1+\nu(\frac{z}{\varepsilon^2})\right)\hat{u}^\varepsilon=0 \tag{3.1}$$

$$\frac{\partial\hat{u}^\varepsilon}{\partial z}+\frac{i\omega}{\varepsilon}\left(1+\eta(\frac{z}{\varepsilon^2})\right)\hat{p}^\varepsilon=0 \tag{3.2}$$

We can decompose the wave into *right-going modes* A^ε and *left-going modes* B^ε

$$A^\varepsilon(\omega,z)=\frac{1}{2}\left(\hat{p}^\varepsilon(\omega,z)+\hat{u}^\varepsilon(\omega,z)\right),\qquad B^\varepsilon(\omega,z)=\frac{1}{2}\left(\hat{p}^\varepsilon(\omega,z)-\hat{u}^\varepsilon(\omega,z)\right), \tag{3.3}$$

and we look at the waves along the *frequency-dependent characteristics* defined by

$$a^\varepsilon(\omega,z)=A^\varepsilon(\omega,z)\exp\left(\frac{i\omega z}{\varepsilon}\right),\qquad b^\varepsilon(\omega,z)=B^\varepsilon(\omega,z)\exp\left(-\frac{i\omega z}{\varepsilon}\right). \tag{3.4}$$

$(a^\varepsilon, b^\varepsilon)$ satisfy the linear equation

$$\frac{\partial}{\partial z}\begin{pmatrix}a^\varepsilon\\ b^\varepsilon\end{pmatrix}(\omega,z)=Q^\varepsilon(\omega,z)\begin{pmatrix}a^\varepsilon\\ b^\varepsilon\end{pmatrix}(\omega,z). \tag{3.5}$$

where the complex 2×2 matrix Q^ε is given by:

$$Q^\varepsilon(\omega,z)=\frac{i\omega}{2}\begin{pmatrix}-m^\varepsilon(z) & -n^\varepsilon(z)e^{\frac{2i\omega z}{\varepsilon}}\\ n^\varepsilon(z)e^{-\frac{2i\omega z}{\varepsilon}} & m^\varepsilon(z)\end{pmatrix} \tag{3.6}$$

with

$$m(z)=\eta(z)+\nu(z),\qquad n(z)=\eta(z)-\nu(z) \tag{3.7}$$

$$m^\varepsilon(z)=\frac{1}{\varepsilon}m(\frac{z}{\varepsilon^2}),\qquad n^\varepsilon(z)=\frac{1}{\varepsilon}n(\frac{z}{\varepsilon^2}) \tag{3.8}$$

3.2. Boundary values. We assume that a left-going pulse is incoming from the right and is scattered into a reflected wave at $z=0$ and a transmitted wave at $z=-L$ (see Figure 3.1).

The incoming pulse shape is given by the pressure function $f(\frac{t}{\varepsilon})$ where f is assumed to be a L^1 function compactly supported in the Fourier domain:

$$u_{inc}(t, z=0) = -\int \hat{f}(\omega) \exp(\frac{i\omega t}{\varepsilon}) d\omega$$
$$p_{inc}(t, z=0) = \int \hat{f}(\omega) \exp(\frac{i\omega t}{\varepsilon}) d\omega$$
$$\hat{f}(\omega) = \frac{1}{2\pi} \int f(t) \exp(-i\omega t) dt$$

We also impose a radiation condition at $-L$ corresponding to the absence of right-going wave at the left hand-side of the slab $[-L, 0]$. The two-point boundary value problem consisting of the system (3.5) for $z \in [0, L]$ together with the conditions:

$$b^\varepsilon(\omega, z=0) = \hat{f}(\omega), \quad a^\varepsilon(\omega, z=-L) = 0$$

is then well-posed.

3.3. Propagator. It is convenient to transform the two-point boundary value problem into an initial value problem by introducing the propagator $Y^\varepsilon(\omega, -L, z)$ which is a complex 2×2 matrix solution of

$$\frac{\partial Y^\varepsilon}{\partial z}(\omega, -L, z) = Q^\varepsilon(\omega, z) Y^\varepsilon(\omega, -L, z), \quad Y^\varepsilon(\omega, -L, z=-L) = Id_{\mathbb{C}^2}$$

such that

$$Y^\varepsilon(\omega, -L, z) \begin{pmatrix} a^\varepsilon(\omega, -L) \\ b^\varepsilon(\omega, -L) \end{pmatrix} = \begin{pmatrix} a^\varepsilon(\omega, z) \\ b^\varepsilon(\omega, z) \end{pmatrix}.$$

By the form (3.6) of the matrix Q^ε, if the column vector $(a_1^\varepsilon, b_1^\varepsilon)^T$ is solution of equation (3.5) with the initial conditions:

$$a_1^\varepsilon(\omega, -L) = 1, \quad b_1^\varepsilon(\omega, -L) = 0, \tag{3.9}$$

then the column vector $(\overline{b_1^\varepsilon}, \overline{a_1^\varepsilon})^T$ is another solution linearly independent of the first solution, so that the propagator matrix Y^ε can be written as:

$$Y^\varepsilon(\omega, -L, z) = \begin{pmatrix} a_1^\varepsilon & \overline{b_1^\varepsilon} \\ b_1^\varepsilon & \overline{a_1^\varepsilon} \end{pmatrix} (\omega, z).$$

Note also that the matrix Q^ε has zero trace, so that the determinant of Y^ε is conserved and $(a_1^\varepsilon, b_1^\varepsilon)$ satisfies the relation:

$$\det Y^\varepsilon = |a_1^\varepsilon|^2 - |b_1^\varepsilon|^2 = 1. \tag{3.10}$$

We can now define the *transmission and reflection coefficients* $T^\varepsilon(\omega, -L, z)$ and $R^\varepsilon(\omega, -L, z)$, respectively, for a slab $[-L, z]$ by (see also Figure 3.2):

$$Y^\varepsilon(\omega, -L, z) \begin{pmatrix} 0 \\ T^\varepsilon(\omega, -L, z) \end{pmatrix} = \begin{pmatrix} R^\varepsilon(\omega, -L, z) \\ 1 \end{pmatrix}.$$

In terms of the propagator entries they are given by:

$$R^\varepsilon(\omega, -L, z) = \frac{\overline{b_1^\varepsilon}}{\overline{a_1^\varepsilon}}(\omega, z), \quad T^\varepsilon(\omega, -L, z) = \frac{1}{\overline{a_1^\varepsilon}}(\omega, z)$$

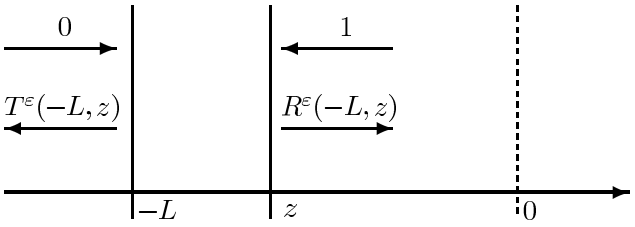

FIG. 3.2. *Reflection and transmission coefficients.*

and they satisfy the closed form nonlinear differential system:

$$\frac{\partial R^\varepsilon}{\partial z} = -i\omega m^\varepsilon(z)R^\varepsilon - \frac{i\omega}{2}e^{-\frac{2i\omega z}{\varepsilon}}n^\varepsilon(z)(R^\varepsilon)^2 - \frac{i\omega}{2}e^{\frac{2i\omega z}{\varepsilon}}n^\varepsilon(z), \tag{3.11}$$

$$\frac{\partial T^\varepsilon}{\partial z} = -\frac{i\omega}{2}T^\varepsilon\left(e^{-\frac{2i\omega z}{\varepsilon}}n^\varepsilon(z)R^\varepsilon + m^\varepsilon(z)\right), \tag{3.12}$$

with the initial conditions at $z=-L$:

$$R^\varepsilon(\omega,-L,z=-L)=0, \quad T^\varepsilon(\omega,-L,z=-L)=1.$$

Note that Eq. (3.10) implies the conservation of energy relation

$$|R^\varepsilon|^2+|T^\varepsilon|^2=1 \tag{3.13}$$

and in turn the uniform boundedness of the transmission and reflection coefficients. Note also that R^ε and T^ε are the reflection and transmission coefficients for the modified characteristics (3.4). In terms of the real characteristics the reflection and transmission coefficients are R^ε and $T^\varepsilon\exp(-i\omega L/\varepsilon)$, respectively.

3.4. Quantities of interest. The transmitted wave at time t, denoted by (u_{tr},p_{tr}), is the left-going wave which admits the following integral representation i n terms of the transmission coefficients:

$$u_{tr}(t,z=-L) = -\int \hat{f}(\omega)T^\varepsilon(\omega,-L,0)\exp\left(\frac{i\omega(t-L)}{\varepsilon}\right)d\omega, \tag{3.14}$$

$$p_{tr}(t,z=-L) = \int \hat{f}(\omega)T^\varepsilon(\omega,-L,0)\exp\left(\frac{i\omega(t-L)}{\varepsilon}\right)d\omega. \tag{3.15}$$

The reflected wave at time t, denoted by (u_{ref},p_{ref}), is the right-going wave which admits the following integral representation in terms of the reflection coefficients:

$$u_{ref}(t,z=0) = \int \hat{f}(\omega)R^\varepsilon(\omega,-L,0)\exp\left(\frac{i\omega t}{\varepsilon}\right)d\omega, \tag{3.16}$$

$$p_{ref}(t,z=0) = \int \hat{f}(\omega)R^\varepsilon(\omega,-L,0)\exp\left(\frac{i\omega L}{\varepsilon}\right)d\omega. \tag{3.17}$$

4. Transmitted front wave. Before going into time reversal we give an integral representation for the *coherent transmitted wave front* observed at $z=-L$ around the expected arrival time L. By Eq. (3.15), the transmitted front observed in the time scale of the initial pulse is given by:

$$p_{tr}(L+\varepsilon t,z=-L) = \int e^{i\omega t}\hat{f}(\omega)T^\varepsilon(\omega,-L,0)d\omega. \tag{4.1}$$

The transmission coefficients are given by $T^\varepsilon(\omega,-L,0)=1/\overline{a_1^\varepsilon}(\omega,0)$ where a_1^ε satisfies (3.5) with the initial conditions (3.9). The limit of p_{tr} has been derived in [22]. The process $(p_{tr}(L+\varepsilon t, z=-L))_{t\in(-\infty,+\infty)}$ converges in the space of the continuous and bounded functions to

$$P_{tr}(t)=\int \hat{f}(\omega)\exp\left(i\omega(t-\frac{\sqrt{\alpha_m}}{\sqrt{2}}B_L)-\frac{\alpha_n\omega^2}{4}L\right)d\omega,$$

where B_L is a standard Brownian motion and

$$\alpha_m=\int_0^\infty \mathbb{E}[m(0)m(z)]dz, \qquad \alpha_n=\int_0^\infty \mathbb{E}[n(0)n(z)]dz, \tag{4.2}$$

Using convolution operators the transmitted front can be written in a simpler form:

$$P_{tr}(t)=f*K\left(t-\frac{\sqrt{\alpha_m}}{\sqrt{2}}B_L\right), \tag{4.3}$$

which means that a random Gaussian centering appears through the Brownian motion B_L while the pulse shape spreads in a deterministic way through the convolution by the Gaussian kernel K whose Fourier transform is

$$\hat{K}(\omega)=\exp\left(-\frac{\alpha_n\omega^2 L}{4}\right).$$

Note that the parameter α_m imposes the random time shift, while the parameter α_n imposes the deterministic reshaping of the pulse. This result corresponds to the O'Doherty-Anstey (ODA) theory celebrated in geophysics [16].

5. Time reversal in reflection (TRR). The first step of the time reversal procedure consists in recording the reflected signal at $z=0$ up to a certain time. During this first part of the experiment the fluctuations of the medium are represented by the processes η_i, ν_i, and the sum and difference by m_i and n_i, respectively. It turns out that as $\varepsilon\to 0$ the interesting asymptotic regime arises when we record the signal up to a large time of order 1 which we denote by t_1 with $t_1>0$. In the next step of the time reversal procedure a piece of the recorded signal is cut using a cut-off function $s\mapsto G_{t_1}(s)$ where the support of G_{t_1} is included in $[0,t_1]$:

$$p_{ref,cut}(t)=p_{ref}(t)G_{t_1}(t).$$

One then time reverses that piece of signal and sends it back into the medium. Observe that the part of the wave which came in last will go out first. We also change the sign of the recorded velocity so as to generate a pure left-going wave. The time-reversed pressure wave sent back into the medium is given by:

$$\begin{aligned} p_{inc(TRR)}(t,z=0) &= p_{ref}(t_1-t)G_{t_1}(t_1-t) \\ &= \frac{1}{\varepsilon}\int\int \exp\left(\frac{i\omega(t_1-t)}{\varepsilon}\right)\hat{p}^\varepsilon_{ref}(\omega')\hat{G}_{t_1}(\frac{\omega-\omega'}{\varepsilon})d\omega' d\omega \end{aligned}$$

where $\hat{G}_{t_1}$ is the Fourier transform of G_{t_1}:

$$\hat{G}_{t_1}(\omega)=\frac{1}{2\pi}\int G_{t_1}(t)\exp(-i\omega t)dt$$

Using the fact that $p_{inc(TRR)}$ is real valued:

$$p_{inc(TRR)}(t,z=0)=\frac{1}{\varepsilon}\int\int\exp\left(\frac{i\omega(t-t_1)}{\varepsilon}\right)\overline{\hat{p}^{\varepsilon}_{ref}}(\omega')\overline{\hat{G}}_{t_1}(\frac{\omega-\omega'}{\varepsilon})d\omega' d\omega,$$

where TRR stands for "Time Reversal in Reflection". The fluctuations of the medium may have been modified between the time windows corresponding to the first and second parts of the time-reversal experiment. We shall denote by (η_{ii},ν_{ii}) the random process that represents the fluctuations of the medium during the second part of the time-reversal experiment. We also denote by m_{ii} and n_{ii} their sum and difference. (η_{ii},ν_{ii}) is assumed to have the same statistical distribution as (η_i,ν_i), but they are different realizations and we shall see that the impact of this difference will be characterized by a correlation degree between the processes (η_i,ν_i) and (η_{ii},ν_{ii}).

This new incoming signal re-propagates into the medium (η_{ii},ν_{ii}), and generates a new reflected signal which we observe at the time $t_2+\varepsilon t$, that is, around the time t_2 in the scale of the initial pulse. In terms of the reflection coefficients R^{ε}_{ii} associated with the medium (η_{ii},ν_{ii}), the observed reflected signal is given by

$$p_{ref(TRR)}(t_2+\varepsilon t,z=0)=\int\hat{p}^{\varepsilon}_{inc(TR)}(\omega)R^{\varepsilon}_{ii}(\omega,-L,0)e^{\frac{i\omega t_2}{\varepsilon}+i\omega t}d\omega.$$

Substituting the expression of $\hat{p}^{\varepsilon}_{inc(TRR)}$ into this equation yields the following representation of the reflected signal:

$$p_{ref(TRR)}(t_2+\varepsilon t,z=0)=\frac{1}{\varepsilon}\int\int e^{i\omega t}e^{\frac{i\omega(t_2-t_1)}{\varepsilon}}\overline{\hat{f}}(\omega')\overline{\hat{G}}_{t_1}(\frac{\omega-\omega'}{\varepsilon})$$
$$\times R^{\varepsilon}_{ii}(\omega,-L,0)\overline{R^{\varepsilon}_{i}}(\omega',-L,0)d\omega' d\omega.$$

After the change of variable $\omega'=\omega-\varepsilon h$ the representation becomes

$$p_{ref(TRR)}(t_2+\varepsilon t,z=0)=\int\int e^{i\omega t}e^{\frac{i\omega(t_2-t_1)}{\varepsilon}}\overline{\hat{f}}(\omega-\varepsilon h)\overline{\hat{G}}_{t_1}(h)$$
$$\times R^{\varepsilon}_{ii}(\omega,-L,0)\overline{R^{\varepsilon}_{i}}(\omega-\varepsilon h,-L,0)dh\,d\omega. \tag{5.1}$$

Note that by Eq. (3.13) the reflection coefficients are bounded and we shall show that the rapid phase $\exp(i\omega(t_2-t_1)/\varepsilon)$ averages out the integral except when $t_2=t_1$. This means that refocusing can be observed only at the time $t_2=t_1$. The precise description of the refocused pulse will be carried out in Section 7.4.

6. Time reversal in transmission (TRT). The time reversal procedure consists in recording the transmitted signal at $z=-L$ over the time interval $[L+t_0,L+t_1]$. During this first part of the experiment the fluctuations of the medium is represented by the process m_i. A piece of the recorded signal is cut using a cut-off function $s\mapsto G_{t_0,t_1}(s-L)$ where the support of G_{t_0,t_1} is included in $[t_0,t_1]$:

$$p_{tr,cut}(t)=p^{\varepsilon}_{tr}(L+t,z=-L)G_{t_0,t_1}(t).$$

One then time reverses that piece of signal and sends it back into the medium by changing the sign of the velocity, so that we generate a right-going wave. The pressure sent back is given by

$$p_{inc(TRT)}(t,z=-L)=p_{tr}(L+t_1-t,z=-L)G_{t_0,t_1}\,(t_1-t)$$
$$=\frac{1}{\varepsilon}\int\int\exp\left(\frac{i\omega(t_1-t)}{\varepsilon}\right)\hat{p}^{\varepsilon}_{tr}(\omega')\hat{G}_{t_0,t_1}(\frac{\omega-\omega'}{\varepsilon})d\omega' d\omega$$

FIG. 6.1. *Adjoint reflection and transmission coefficients for time reversal.*

where $\hat{p}^{\varepsilon}_{tr}$ is the scaled Fourier transform of the shifted received signal $t \mapsto p_{tr}(L + t, z = -L)$:

$$\hat{p}^{\varepsilon}_{tr}(\omega) = \hat{f}(\omega) T^{\varepsilon}_{i}(\omega, -L, 0)$$

and T^{ε}_{i} is the transmission coefficient associated with the fluctuations (η_i, ν_i). Since it is real-valued $p_{inc(TRT)}$ also reads as:

$$p_{inc(TRT)}(t, z = -L) = \frac{1}{\varepsilon} \int \int \exp\left(\frac{i\omega(t - t_1)}{\varepsilon}\right) \overline{\hat{p}^{\varepsilon}_{tr}}(\omega') \overline{\hat{G}}_{t_0,t_1}(\frac{\omega - \omega'}{\varepsilon}) d\omega' d\omega.$$

The fluctuations of the medium may have been modified between the time windows corresponding to the first and second parts of the time-reversal experiment. We shall denote by (η_{ii}, ν_{ii}) the random process that represents the fluctuations of the medium during the second part of the time-reversal experiment. (η_{ii}, ν_{ii}) is assumed to have the same statistical distribution as (η_i, ν_i), but they are different and we shall see that the impact of this difference will be characterized by a correlation degree between the processes (η_i, ν_i) and (η_{ii}, ν_{ii}).

Let us denote by $\tilde{R}^{\varepsilon}_{ii}$ and $\tilde{T}^{\varepsilon}_{ii}$ the reflection and transmission coefficients for the experiment corresponding to a right-going input wave incoming from the left (see Figure 6.1). Using the propagator Y^{ε}_{ii} defined as in Section 3.3 with the process (η_{ii}, ν_{ii}), $\tilde{R}^{\varepsilon}_{ii}$ and $\tilde{T}^{\varepsilon}_{ii}$ obey the relation

$$Y^{\varepsilon}_{ii}(\omega, -L, 0) \begin{pmatrix} 1 \\ \tilde{R}^{\varepsilon}_{ii}(\omega, -L, 0) \end{pmatrix} = \begin{pmatrix} \tilde{T}^{\varepsilon}_{ii}(\omega, -L, 0) \\ 0 \end{pmatrix}.$$

In terms of the propagator entries they are given by:

$$\tilde{R}^{\varepsilon}_{ii}(\omega, -L, 0) = -\frac{b^{\varepsilon}_{1,ii}}{a^{\varepsilon}_{1,ii}}(\omega, 0), \qquad \tilde{T}^{\varepsilon}_{ii}(\omega, -L, 0) = \frac{1}{a^{\varepsilon}_{1,ii}}(\omega, 0)$$

which shows that

$$\tilde{T}^{\varepsilon}_{ii}(\omega, -L, 0) = T^{\varepsilon}_{ii}(\omega, -L, 0).$$

Accordingly, the new incoming signal propagates into the medium m_{ii}, and generates a new transmitted signal which we observe at the time $t_2 + \varepsilon t$ that is around the time t_2 in the scale of the initial pulse. In terms of the transmission coefficients T^{ε}_{ii} associated the process (η_{ii}, ν_{ii}), the observed transmitted signal is given by

$$p_{tr(TRT)}(t_2 + \varepsilon t, z = 0) = \int \hat{p}^{\varepsilon}_{inc(TRT)}(\omega) T^{\varepsilon}_{ii}(\omega, -L, 0) e^{\frac{i\omega t_2}{\varepsilon} + i\omega t - i\omega \frac{L}{\varepsilon}} d\omega.$$

Substituting the expression of $\hat{p}^{\varepsilon}_{inc(TRT)}$ into this equation yields the following representation of the new transmitted signal

$$p_{tr(TRT)}(t_2+\varepsilon t, z=0) = \frac{1}{\varepsilon}\int\int e^{i\omega t} e^{\frac{i\omega(t_2-t_1-L)}{\varepsilon}} \overline{\hat{f}}(\omega')\overline{\hat{G}}_{t_0,t_1}(\frac{\omega-\omega'}{\varepsilon}) \times T^{\varepsilon}_{ii}(\omega,-L,0)\overline{T^{\varepsilon}_{i}}(\omega',-L,0)d\omega' d\omega.$$

After the change of variable $\omega' = \omega - \varepsilon h$ the representation becomes

$$p_{tr(TRT)}(t_2+\varepsilon t, z=0) = \int\int e^{i\omega t} e^{\frac{i\omega(t_2-t_1-L)}{\varepsilon}} \overline{\hat{f}}(\omega-\varepsilon h)\overline{\hat{G}}_{t_0,t_1}(h) \times T^{\varepsilon}_{ii}(\omega,-L,0)\overline{T^{\varepsilon}_{i}}(\omega-\varepsilon h,-L,0)dh\, d\omega. \tag{6.1}$$

The precise asymptotics of the transmitted wave will be carried out in the next section. It is easily seen that the refocusing will only take place if $t_2 = L + t_1$ due to the fast phase.

7. The refocused pulse for Time Reversal in Reflection. The refocused pulse is given by

$$p_{ref(TRR)}(t_1+\varepsilon t, z=0) = \int\int e^{i\omega t} e^{i\varepsilon h t/2} \overline{\hat{f}}(\omega-\varepsilon h/2)\overline{\hat{G}}_{t_1}(h) \times R^{\varepsilon}_{ii}(\omega+\varepsilon h/2,-L,0)\overline{R^{\varepsilon}_{i}}(\omega-\varepsilon h/2,-L,0)dh\, d\omega. \tag{7.1}$$

This section is devoted to the proof of the convergence of the refocused pulse shape to an effective shape as $\varepsilon \to 0$.

7.1. Tightness. We first address the tightness of the process.

LEMMA 7.1. *The refocused pulse* $\left((p^{\varepsilon}_{ref(TRR)}(t_1+\varepsilon t))_{-\infty<t<\infty}\right)_{\varepsilon>0}$ *is a tight (i.e. weakly compact) family in the space of continuous trajectories equipped with the sup norm.*

Proof. We must show that, for any $\delta > 0$, there exists a compact subset K of the space of continuous bounded functions such that:

$$\sup_{\varepsilon>0} \mathbb{P}(p^{\varepsilon}_{ref(TRR)}(t_1+\varepsilon.) \in K) \geq 1-\delta$$

On the one hand the energy conservation relation (3.13) yields that $p^{\varepsilon}_{ref(TRR)}(t_1+\varepsilon t)$ is uniformly bounded by:

$$|p^{\varepsilon}_{ref(TRR)}(t_1+\varepsilon t)| \leq \int |\hat{f}(\omega)|d\omega \times \int |\hat{G}_{t_1}(h)|d\omega dh \tag{7.2}$$

On the other hand the modulus of continuity

$$M^{\varepsilon}(\delta) = \sup_{|s_1-s_2|\leq\delta} |p^{\varepsilon}_{ref(TRR)}(t_1+\varepsilon s_1) - p^{\varepsilon}_{ref(TRR)}(t_1+\varepsilon s_2)|$$

is bounded by

$$M^{\varepsilon}(\delta) \leq \int \sup_{|s_1-s_2|\leq\delta} |1-\exp(i\omega(s_1-s_2))||\hat{f}(\omega)|d\omega \times \int |\hat{G}_{t_1}(h)|d\omega dh$$

which goes to zero as δ goes to zero uniformly with respect to ε. □

7.2. Convergence of the finite-dimensional distributions. The uniform boundedness (7.2) implies that the finite-dimensional distributions of the process $p^\varepsilon_{ref(TRR)}(t_1+.)$ will be characterized by the moments

$$\mathbb{E}[p^\varepsilon_{ref(TRR)}(t_1+\varepsilon s_1)^{p_1}\dots p^\varepsilon_{ref(TRR)}(t_1+\varepsilon s_k)^{p_k}] \tag{7.3}$$

for every real numbers $s_1<\dots<s_k$ and every integers $p_1,\dots,p_k$.

7.2.1. First moment. Let us first address the first moment. Using the representation (7.1) the expectation of $p^\varepsilon_{ref(TRR)}(t_1+\varepsilon t)$ reads:

$$\begin{aligned}\mathbb{E}[p_{ref(TRR)}(t_1+\varepsilon t)] = \int\int e^{i\omega t}e^{i\varepsilon ht/2}\overline{\hat f}(\omega-\varepsilon h/2)\overline{\hat G}_{t_1}(h)\\ \times\mathbb{E}[R^\varepsilon_{ii}(\omega+\varepsilon h/2,-L,0)\overline{R^\varepsilon_i}(\omega-\varepsilon h/2,-L,0)]dh\,d\omega.\end{aligned} \tag{7.4}$$

As shown by (7.4), the statistical distribution of the refocused pulse will depend on the frequency autocorrelation function of the reflection coefficient. We shall denote:

$$U^\varepsilon_{1,1}(\omega,h,z)=R^\varepsilon_{ii}(\omega+\frac{\varepsilon h}{2},-L,z)\overline{R^\varepsilon_i}(\omega-\frac{\varepsilon h}{2},-L,z)$$

and we shall extend the approach developed in [3, 7]. It is necessary to consider a family of moments so as to get a closed system of equations. We introduce for $q,p\in\mathbb{N}$

$$U^\varepsilon_{q,p}(\omega,h,z)=\left(R^\varepsilon_{ii}(\omega+\frac{\varepsilon h}{2},-L,z)\right)^q\left(\overline{R^\varepsilon_i}(\omega-\frac{\varepsilon h}{2},-L,z)\right)^p$$

Using the Ricatti equation (3.11) satisfied by R^ε, we deduce

$$\begin{aligned}\frac{\partial U^\varepsilon_{q,p}}{\partial z} &= i\omega(pm^\varepsilon_i-qm^\varepsilon_{ii})U^\varepsilon_{q,p}+ie^{\frac{2i\omega z}{\varepsilon}}\frac{\omega}{2}\left(-qn^\varepsilon_{ii}e^{ihz}U^\varepsilon_{q-1,p}+pn^\varepsilon_i e^{-ihz}U^\varepsilon_{q,p+1}\right)\\ &\quad+ie^{-\frac{2i\omega z}{\varepsilon}}\frac{\omega}{2}\left(pn^\varepsilon_i e^{ihz}U^\varepsilon_{q,p-1}-qn^\varepsilon_{ii}e^{-ihz}U^\varepsilon_{q+1,p}\right)\end{aligned}$$

starting from

$$U^\varepsilon_{q,p}(\omega,h,z=-L)=\mathbf{1}_0(q)\mathbf{1}_0(p),$$

where $\mathbf{1}_0(q)=1$ if $q=0$ and 0 otherwise. Taking a shifted scaled Fourier transform with respect to h

$$V^\varepsilon_{q,p}(\omega,\tau,z)=\frac{1}{2\pi}\int e^{ih(\tau-(q+p)z)}U^\varepsilon_{q,p}(\omega,h,z)dh \tag{7.5}$$

we get

$$\begin{aligned}\frac{\partial V^\varepsilon_{q,p}}{\partial z} &= -(q+p)\frac{\partial V^\varepsilon_{q,p}}{\partial\tau}+i\omega(pm^\varepsilon_i-qm^\varepsilon_{ii})V^\varepsilon_{q,p}+i\frac{\omega}{2}e^{\frac{2i\omega z}{\varepsilon}}\left(-qn^\varepsilon_{ii}V^\varepsilon_{q-1,p}+pn^\varepsilon_i V^\varepsilon_{q,p+1}\right)\\ &\quad+ie^{-\frac{2i\omega z}{\varepsilon}}\frac{\omega}{2}\left(pn^\varepsilon_i V^\varepsilon_{q,p-1}-qn^\varepsilon_{ii}V^\varepsilon_{q+1,p}\right)\end{aligned}$$

starting from

$$V^\varepsilon_{q,p}(\omega,\tau,z=-L)=\delta_0(\tau)\mathbf{1}_0(q)\mathbf{1}_0(p).$$

Applying a diffusion-approximation theorem [3, Section 3] establishes that the processes $V^{\varepsilon}_{q,p}$ converge to diffusion processes as $\varepsilon \to 0$. In particular the expectations $\mathbb{E}[V^{\varepsilon}_{p,p}(\omega,\tau,z)]$, $p \in \mathbb{N}$, converge to $v_p(\omega,\tau,z)$ which obey the closed system of transport equations:

$$\frac{\partial v_p}{\partial z} + 2p\frac{\partial v_p}{\partial \tau} = (\mathcal{L}_\omega v)_p - 2\alpha_m(1-\delta_m)\omega^2 p^2 v_p \tag{7.6}$$

$$(\mathcal{L}_\omega \phi)_p = \frac{1}{2}\alpha_n\delta_n\omega^2p^2\left(\phi_{p+1}+\phi_{p-1}-2\phi_p\right) - \alpha_n(1-\delta_n)\omega^2p^2\phi_p \tag{7.7}$$

$$v_p(\omega,\tau,z=-L) = \delta_0(\tau)\mathbf{1}_0(p) \tag{7.8}$$

where

$$\alpha_n = \int_0^\infty \mathbb{E}[n_i(0)n_i(z)]dz = \int_0^\infty \mathbb{E}[n_{ii}(0)n_{ii}(z)]dz \tag{7.9}$$

$$\alpha_m = \int_0^\infty \mathbb{E}[m_i(0)m_i(z)]dz = \int_0^\infty \mathbb{E}[m_{ii}(0)m_{ii}(z)]dz \tag{7.10}$$

$$\delta_n = \frac{1}{\alpha_n}\int_0^\infty \mathbb{E}[n_{ii}(0)n_i(z)]dz = \frac{1}{\alpha_n}\int_0^\infty \mathbb{E}[n_i(0)n_{ii}(z)]dz \tag{7.11}$$

$$\delta_m = \frac{1}{\alpha_m}\int_0^\infty \mathbb{E}[m_{ii}(0)m_i(z)]dz = \frac{1}{\alpha_m}\int_0^\infty \mathbb{E}[m_i(0)m_{ii}(z)]dz \tag{7.12}$$

α_m and α_n are the standard integrated covariances of the processes m and n in absence of time perturbations. δ_m, respectively δ_n, characterizes the correlation degree between the processes m_i and m_{ii}, respectively n_i and n_{ii}. If the fluctuations of the medium are the same in the two steps of the experiment ($m_i \equiv m_{ii}$, $n_i \equiv n_{ii}$), then $\delta_m = \delta_n = 1$, and the limit transport equations (7.6) have the same form as the ones obtained in [3]. If the fluctuations of the medium are completely uncorrelated in the two steps of the experiment ((η_i,ν_i) and (η_{ii},ν_{ii}) independent), then $\delta_m = \delta_n = 0$ so that $v_p(\omega,\tau,z) = \delta_0(\tau)\mathbf{1}_0(p)$.

We then get the limit of the autocorrelation function of the reflection coefficient:

$$\mathbb{E}\left[R^{\varepsilon}_{ii}(\omega+\frac{\varepsilon h}{2},-L,0)\overline{R^{\varepsilon}_{i}}(\omega-\frac{\varepsilon h}{2},-L,0)\right] \overset{\varepsilon\to 0}{\longrightarrow} \int v_1(\omega,\tau,0)e^{-ih\tau}d\tau$$

The quantity $v_1(\omega,\tau,0)$ is obtained through the system of transport equations (7.6). We can rewrite this system by introducing the family of processes :

$$\begin{aligned} &dW_p + 2p\frac{\partial W_p}{\partial \tau}dz = 2ip\omega\sqrt{\alpha_m(1-\delta_m)}W_p \circ dB_z + (\mathcal{L}_\omega W)_p dz \\ &W_p(\omega,\tau,z=-L) = \delta_0(\tau)\mathbf{1}_0(p) \end{aligned} \tag{7.13}$$

driven by a standard Brownian motion B_z. Indeed it is straightforward to check that we have

$$v_p(\omega,\tau,z) = \mathbf{E}[W_p(\omega,\tau,z)]$$

where the expectation $\mathbf{E}$ is taken with respect to the distribution of the Brownian motion B_z. Using this expression of the asymptotic autocorrelation function yields

$$\begin{aligned} \mathbb{E}[p_{ref(TRR)}(t_1+\varepsilon t)] &\overset{\varepsilon\to 0}{\longrightarrow} \int\int\int e^{i\omega t}e^{-ih\tau}\overline{\hat{f}}(\omega)\overline{\hat{G}_{t_1}}(h)\mathbf{E}\left[W_1(\omega,\tau,0)\right]dhd\tau d\omega. \\ &= \int\int e^{i\omega t}\overline{\hat{f}}(\omega)G_{t_1}(\tau)\mathbf{E}\left[W_1(\omega,\tau,0)\right]d\tau d\omega. \end{aligned}$$

7.2.2. Higher order moments. Let us now consider the general moment (7.3). Using the representation (7.1) for each factor $p^{\varepsilon}_{ref(TRR)}(t_1+\varepsilon s_j)$, these moments can be written as multiple integrals over $p=\sum_{j=1}^{k} p_j$ frequencies:

$$\mathbb{E}\left[p^{\varepsilon}_{ref(TRR)}(t_1+\varepsilon s_1)^{p_1}\dots p^{\varepsilon}_{ref(TRR)}(t_1+\varepsilon s_k)^{p_k}\right]=$$

$$\int\dots\int\mathbb{E}\left[\prod_{\substack{1\le j\le k\\ 1\le l\le p_j}} U^{\varepsilon}_{1,1}(\omega_{j,l},h_{j,l},0)\right]\prod_{\substack{1\le j\le k\\ 1\le l\le p_j}}\overline{\hat{f}}(\omega_{j,l})e^{i\omega_{j,l}s_j}e^{i\varepsilon h_{j,l}s_j/2}\overline{\hat{G}_{t_1}}(h_{j,l})d\omega_{j,l}dh_{j,l}$$

The important quantity is $\mathbb{E}\left[\prod_{j,l}U^{\varepsilon}_{1,1}(\omega_{j,l},h_{j,l},0)\right]$. Our problem is now to find the limit, as ε goes to 0, of these moments for k distinct frequencies. This limit will be deduced from the study of the convergence of the distribution of $(U^{\varepsilon}_{q_1,p_1}(\omega_1,h_1,z),\dots,U^{\varepsilon}_{q_k,p_k}(\omega_k,h_k,z))$ which results once again from the application of a diffusion-approximation theorem. Introducing V^{ε} as in Eq. (7.5) it is found that $(V^{\varepsilon}_{q_1,p_1}(\omega_1,\tau_1,z),\dots,V^{\varepsilon}_{q_k,p_k}(\omega_k,\tau_k,z))$ converges as $\varepsilon\to 0$ to a diffusion process. In particular,

$$v_{p_1,\dots,p_k}(\omega_1,\dots,\omega_k,\tau_1,\dots,\tau_k,z):=\lim_{\varepsilon\to 0}\mathbb{E}\left[\prod_j V^{\varepsilon}_{p_j,p_j}(\omega_j,\tau_j,z)\right]$$

is solution of :

$$\frac{\partial v_{p_1,\dots,p_k}}{\partial z}+2\sum_j p_j\frac{\partial v_{p_1,\dots,p_k}}{\partial\tau_j}=\sum_j\mathcal{L}_{\omega_j}v_{p_1,\dots,p_k}-2\alpha_m(1-\delta_m)\left(\sum_j\omega_j p_j\right)^2 v_{p_1,\dots,p_k}$$

$$v_{p_1,\dots,p_k}(\omega_1,\dots,\omega_k,\tau_1,\dots,\tau_k,z=-L)=\prod_j\delta_0(\tau_j)\mathbf{1}_0(p_j)$$

Using the families of processes W introduced in Eq. (7.13) defined for every frequency ω with the same Brownian motion B_z, a direct calculation shows that $\mathbf{E}\left[\prod_j W_{p_j}(\omega_j,\tau_j)\right]$ satisfies the above system, so that we have

$$v_{p_1,\dots,p_k}(\omega_1,\dots,\omega_k,\tau_1,\dots,\tau_k,z)=\mathbf{E}\left[\prod_j W_{p_j}(\omega_j,\tau_j,z)\right]$$

and consequently,

$$\mathbb{E}\left[p^{\varepsilon}_{ref(TRR)}(t_1+\varepsilon s_1)^{p_1}\dots p^{\varepsilon}_{ref(TRR)}(t_1+\varepsilon s_k)^{p_k}\right]\xrightarrow{\varepsilon\to 0}$$

$$\int\dots\int\mathbf{E}\left[\prod_{\substack{1\le j\le k\\ 1\le l\le p_j}} W_1(\omega_{j,l},\tau_{j,l},0)\right]\prod_{\substack{1\le j\le k\\ 1\le l\le p_j}}\overline{\hat{f}}(\omega_{j,l})e^{i\omega_{j,l}s_j}G_{t_1}(\tau_{j,l})d\omega_{j,l}d\tau_{j,l}$$

$$=\mathbf{E}\left[\prod_{1\le j\le k}\left(\int W_1(\omega,\tau,0)\overline{\hat{f}}(\omega)e^{i\omega s_j}G_{t_1}(\tau)d\omega d\tau\right)^{p_j}\right]$$

This shows the convergence of the finite-dimensional distributions of $(p^{\varepsilon}_{ref(TRR)}(t_1 + \varepsilon s))_{s\in(-\infty,\infty)}$ to the ones of

$$\int W_1(\omega,\tau,0)\overline{\hat{f}}(\omega)e^{i\omega s}G_{t_1}(\tau)d\omega d\tau$$

7.3. Convergence of the refocused pulse. We have just demonstrated the tightness of the process $\left(p_{ref(TRR)}(t_1+\varepsilon t, z=0)\right)_{t\in(-\infty,\infty)}$ as well as the convergence of its finite-dimensional distributions. Accordingly this demonstrates the following theorem.

THEOREM 7.2. *The refocused signal* $\left(p_{ref(TRR)}(t_1+\varepsilon t, z=0)\right)_{t\in(-\infty,\infty)}$ *converges in distribution as* $\varepsilon \to 0$ *to*

$$P_{ref(TRR)}(t) = \int \Lambda^L_{ref}(\omega,\tau)\overline{\hat{f}}(\omega)e^{i\omega t}G_{t_1}(\tau)d\omega d\tau$$

where $\Lambda^L_{ref}(\omega,\tau) = W_1(\omega,\tau,0)$ *is the random density given by the system (7.13). We can also write that*

$$P_{ref(TRR)}(t) = \left(f(-\,\cdot) * K_{TRR}(\cdot)\right)(t).$$

The Fourier transform of the kernel K_{TRR} *is the convolution of the time-inverted cut-off function* G_{t_1} *with the density* $\tau \mapsto \Lambda^L_{ref}(\omega,\tau)$ *evaluated at* 0*:*

$$\hat{K}_{TRR}(\omega) = \left(G_{t_1}(-\,\cdot) * \Lambda^L_{ref}(\omega,\cdot)\right)(0) = \int G_{t_1}(\tau)\Lambda^L_{ref}(\omega,\tau)d\tau.$$

We can give a probabilistic representation of the density Λ^L_{ref} in terms of a jump Markov process. Let us introduce the process $(X_t)_{t\geq 0}$ with state space $\mathbb{N}\cup\{\partial\}$ (where ∂ is the cemetery state) and infinitesimal generator $\mathcal{L}_\omega$ given by (7.7). Note that, as soon as $\delta_n < 1$, the jump process can be killed. When the jump process reaches the state $x \in \mathbb{N}^*$, a random clock with exponential distribution and mean $\tau(\omega,x) = (x^2\alpha_n\omega^2)^{-1}$ starts running. When the clock strikes, the process is killed and goes to ∂ with probability $p_\partial = 1-\delta_n$, it jumps to $x+1$ with probability $p_+ = \delta_n/2$, and to $x-1$ with probability $p_- = p_+$. Finally, 0 is an absorbing state. This representation of a system of transport equations in terms of a canonical Markov process was first introduced in [3], and it turns out that we can extend this idea to the system (7.13) by means of a Feynman-Kac formula. After some algebra we get

$$\begin{aligned}\int_{\tau_0}^{\tau_1} W_1(\omega,\tau,0)d\tau = \mathbb{E}_1\Big[&\mathbf{1}_{\int_0^L 2X_s ds\in[\tau_0,\tau_1]}\mathbf{1}_{X_L=0}\\ &\times\exp\left(2i\sqrt{\alpha_m(1-\delta_m)}\omega\int_0^L X_s dB_s\right)\Big]\end{aligned} \tag{7.14}$$

where $\mathbb{E}_{x_0}$ stands for the expectation over the distribution of the jump process starting from $X_0 = x_0$ (the expectation is *not* taken with respect to the distribution of the Brownian motion B).

The refocused pulse shape has thus a random shape in presence of time perturbations of the medium fluctuations. There is no more statistical stability as there used to be in the standard configurations where the medium is time-independent [9].

7.4. Pulse stabilization for a particular class of perturbations. The main result of this section is the refocusing of the pulse with a deterministic shape in the particular case $\delta_m = 0$. The process W_1 is then deterministic, hence the density Λ^L_{ref} is also deterministic. The configuration $\delta_m = 1$ occurs when the time-perturbation affects both the density ρ (through the process ν) and the bulk modulus K (through the process η), but the process $m = \eta + \nu$ is not perturbed so that $m_i = m_{ii}$. This means roughly speaking that the local velocity is not affected by the time-perturbation. For instance this occurs if $\eta = -\nu$, since this implies $m_i = m_{ii} \equiv 0$.

THEOREM 7.3. *If $\delta_m = 1$, then the signal $\left(p_{ref(TRR)}(t_1 + \varepsilon t, z = 0)\right)_{t\in(-\infty,\infty)}$ converges in probability to $P_{ref(TRR)}(t)$ as $\varepsilon \to 0$ where $P_{ref(TRR)}$ is the deterministic pulse shape:*

$$P_{ref(TRR)}(t) = \left(f(-\,\cdot) * K_{TRR}(\cdot)\right)(t).$$

The Fourier transform of the kernel K_{TRR} is the convolution of the time-inverted cut-off function G_{t_1} with the density $\tau \mapsto \Lambda^L_{ref}(\omega, \tau)$ evaluated at 0:

$$\hat{K}_{TRR}(\omega) = \left(G_{t_1}(-\,\cdot) * \Lambda^L_{ref}(\omega, \cdot)\right)(0) = \int G_{t_1}(\tau)\Lambda^L_{ref}(\omega, \tau)d\tau.$$

7.5. Analysis of the refocused pulse shape. The explicit description of the refocused pulse shape allows us to perform explicit calculations. For instance, we can compute the mean pulse shape:

$$\mathbb{E}[P_{ref(TRR)}(t)] = \left(f(-\,\cdot) * \mathbb{E}[K_{TRR}](\cdot)\right)(t)$$

$$\mathbb{E}[\hat{K}_{TRR}](\omega) = \int G_{t_1}(\tau)\mathbb{E}[\Lambda^L_{ref}](\omega, \tau)d\tau$$

We shall now address the case of a semi-finite slab $L \to \infty$. This case leads to some simple analytical results. In particular, long but straightforward calculations establish that

$$\mathbb{E}[W_n](\omega, \tau, 0) = \frac{\partial}{\partial u}\left[\left(\frac{\delta_0 \tanh\left(\sqrt{1-\delta_0^2}u\right)}{\sqrt{1-\delta_0^2} + \tanh\left(\sqrt{1-\delta_0^2}u\right)}\right)^n\right]\Bigg|_{u=\alpha_0\omega^2\tau/4}$$

where

$$\alpha_0 = \alpha_n + 2(1-\delta_m)\alpha_m, \qquad \delta_0 = \frac{\delta_n\alpha_n}{\alpha_n + 2(1-\delta_m)\alpha_m} \tag{7.15}$$

We thus get a closed form expression of the expectation of the density

$$\mathbb{E}[\Lambda^{L\to\infty}_{ref}](\omega, \tau) = \frac{\alpha_0\omega^2\delta_0}{4}\frac{1 - \tanh^2\left(\frac{\sqrt{1-\delta_0^2}\alpha_0\omega^2\tau}{4}\right)}{\left[1 + \frac{1}{\sqrt{1-\delta_0^2}}\tanh\left(\frac{\sqrt{1-\delta_0^2}\alpha_0\omega^2\tau}{4}\right)\right]^2} \tag{7.16}$$

Note that in the particular case $\delta_m = 1$, we are actually discussing the deterministic convolution kernel that gives the refocused pulse shape. In that case $\delta_0 = \delta_n$ and $\alpha_0 = \alpha_n$ and all the expectations can be removed from the forthcoming expressions.

Total record. Assume that we record everything at the mirror, so that $G_{t_1} \equiv 1$. In these conditions

$$\mathbb{E}[\hat{K}_{TRR}](\omega) = \frac{1-\sqrt{1-\delta_0^2}}{\delta_0}$$

If the medium is constant during the time reversal experiment $(\eta_i, \nu_i) = (\eta_{ii}, \nu_{ii})$, then $\delta_n = \delta_m = 1$ and $\hat{K}_{TRR}(\omega) \equiv 1$. This is of course expected: The pulse has been completely scattered back by the random half-space due to Anderson localization [17], and we have sent back everything that has been recorder, so we get a perfect refocusing as a result of the time-reversibility of the wave equation.
If the medium has changed between the two parts of the experiment, then $\mathbb{E}[\hat{K}_{TRR}](\omega)$ is equal to the constant G_{TRR} that is strictly less than 1:

$$G_{TRR} = \frac{1-\sqrt{1-\delta_0^2}}{\delta_0}. \tag{7.17}$$

This means that *the mean refocused pulse has exactly the original pulse shape*, up to the attenuation factor G_{TRR} that depends only on the correlation degree δ_0. Note that in this configuration all frequency modes are reflected back whatever the realization of the medium due to the localization effect. The attenuation factor G_{TRR} means that, in the case of a time-dependent random medium, only a part of the reflected wave contributes to the refocused pulse shape. The attenuation factor G_{TRR} is very sensitive to a change of the medium: a mismatch of 1% (resp. 5%) leads to a reduction of 13% (resp. 28%) of the amplitude of the refocused pulse (see figure 7.1a).

Partial record. Assume now that we record only a piece of the reflected signal at the mirror, with a square cut-off function $G_{t_1}(t) = \mathbf{1}_{[0,t_1]}(t)$. If the medium is constant during the time reversal experiment $(\eta_i, \nu_i) = (\eta_{ii}, \nu_{ii})$, then $\delta_m = \delta_n = 1$ and

$$\hat{K}_{TRR}(\omega) = \frac{\alpha_n \omega^2 t_1}{4 + \alpha_n \omega^2 t_1} \tag{7.18}$$

The refocused pulse is a filtered version of the original pulse shape with a high-band filter. The cut-off frequency of the filter is

$$\omega_c = \frac{2}{\sqrt{\alpha_n t_1}}$$

If the medium has changed between the two parts of the experiment, then $\mathbb{E}[\hat{K}_{TRR}](\omega)$ is a function of $\alpha_0\omega^2 t_1$ and δ_0:

$$\mathbb{E}[\hat{K}_{TRR}](\omega) = \delta_0 \frac{\tanh\left(\frac{\sqrt{1-\delta_0^2}\alpha_0\omega^2 t_1}{4}\right)}{\sqrt{1-\delta_0^2} + \tanh\left(\frac{\sqrt{1-\delta_0^2}\alpha_0\omega^2 t_1}{4}\right)} \tag{7.19}$$

For low frequencies, we have

$$\mathbb{E}[\hat{K}_{TRR}](\omega) \overset{\omega \ll \omega_c}{\simeq} \delta_0 \frac{\alpha_0 \omega^2 t_1}{4}$$

which means that we have a reduction by a factor δ_0 w.r.t. the constant configuration. Accordingly, if the frequency content of the initial pulse is in the low-frequency band

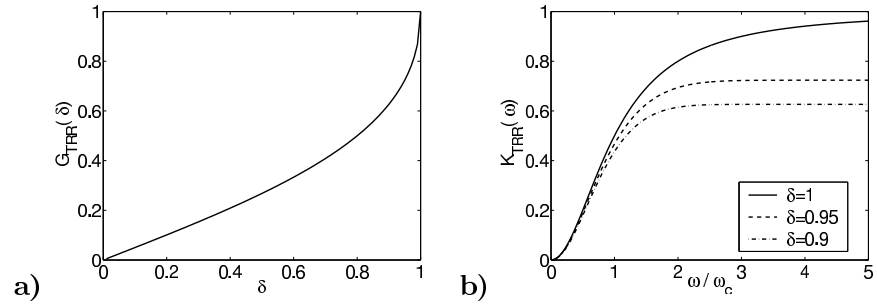

FIG. 7.1. *Picture a: Attenuation factor G_{TRR} as a function of the correlation degree δ (total record). Picture b: Mean filter $\mathbb{E}[\hat{K}_{TRR}]$ as a function of the frequency ω for different correlation degrees (partial record, square cut-off function $G_{t_1}(t) = \mathbf{1}_{[0,t_1]}(t)$). Here $\omega_c = 2/\sqrt{\alpha_0 t_1}$.*

(below ω_c), then the refocused pulse has the original pulse shape, up to the attenuation factor δ_0.
For high frequencies, we have

$$\mathbb{E}[\hat{K}_{TRR}](\omega) \overset{\omega \gg \omega_c}{\simeq} \frac{1-\sqrt{1-\delta_0^2}}{\delta_0}$$

that is to say we recover the case of the semi-infinite slab. This is not surprising: the high-frequencies are those which are scattered back very early, at the beginning of the slab, so they probe the slab as if it were semi-infinite. Note that the attenuation factor for high-frequencies (plotted in Fig. 7.1a) is much stronger than the attenuation factor for low frequencies (which is simply δ_n). This can be seen in Fig. 7.1b where the low frequencies are almost recovered as in the time-independent case, while the high-frequencies are dramatically attenuated. Once again, the high-frequencies are reflected back, but part of this reflected wave does not contribute coherently to the refocused pulse shape.

8. The refocused pulse for Time Reversal in Transmission.

8.1. The autocorrelation function of the transmission coefficient. We study here the autocorrelation function of the transmission coefficient at two nearby frequencies. We first define a new family of processes indexed by $q, p \in \mathbb{N}$

$$\tilde{U}^{\varepsilon}_{q,p}(\omega, h, z) = U^{\varepsilon}_{q,p}(\omega, h, z) T^{\varepsilon}_{ii}(\omega + \frac{\varepsilon h}{2}, -L, z) \overline{T^{\varepsilon}_{i}}(\omega - \frac{\varepsilon h}{2}, -L, z)$$

which satisfy

$$\begin{aligned}
\frac{\partial \tilde{U}^{\varepsilon}_{q,p}}{\partial z} = & i\omega \left((p+\frac{1}{2}) m^{\varepsilon}_{i} - (q+\frac{1}{2}) m^{\varepsilon}_{ii} \right) \tilde{U}^{\varepsilon}_{q,p} \\
& + i e^{\frac{2i\omega z}{\varepsilon}} \frac{\omega}{2} \left(-q n^{\varepsilon}_{ii} e^{ihz} \tilde{U}^{\varepsilon}_{q-1,p} + (p+1) n^{\varepsilon}_{i} e^{-ihz} \tilde{U}^{\varepsilon}_{q,p+1} \right) \\
& + i e^{-\frac{2i\omega z}{\varepsilon}} \frac{\omega}{2} \left(p n^{\varepsilon}_{i} e^{ihz} \tilde{U}^{\varepsilon}_{q,p-1} - (q+1) n^{\varepsilon}_{ii} e^{-ihz} \tilde{U}^{\varepsilon}_{q+1,p} \right)
\end{aligned}$$

starting from

$$\tilde{U}^{\varepsilon}_{q,p}(\omega, h, z = -L) = \mathbf{1}_0(q) \mathbf{1}_0(p).$$

Taking a shifted scaled Fourier transform with respect to h

$$\tilde{V}^{\varepsilon}_{q,p}(\omega,\tau,z)=\frac{1}{2\pi}\int e^{ih(\tau-(q+p)z)}\tilde{U}^{\varepsilon}_{q,p}(\omega,h,z)dh$$

we get

$$\begin{aligned}\frac{\partial\tilde{V}^{\varepsilon}_{q,p}}{\partial z}=&-(q+p)\frac{\partial\tilde{V}^{\varepsilon}_{q,p}}{\partial\tau}+i\omega\left((p+\frac{1}{2})m^{\varepsilon}_{i}-(q+\frac{1}{2})m^{\varepsilon}_{ii}\right)\tilde{V}^{\varepsilon}_{q,p}\\&+ie^{\frac{2i\omega z}{\varepsilon}}\frac{\omega}{2}\left(-qn^{\varepsilon}_{ii}\tilde{V}^{\varepsilon}_{q-1,p}+(p+1)n^{\varepsilon}_{i}\tilde{V}^{\varepsilon}_{q,p+1}\right)\\&+ie^{-\frac{2i\omega z}{\varepsilon}}\frac{\omega}{2}\left(pn^{\varepsilon}_{i}\tilde{V}^{\varepsilon}_{q,p-1}-(q+1)n^{\varepsilon}_{ii}\tilde{V}^{\varepsilon}_{q+1,p}\right)\end{aligned}$$

starting from

$$\tilde{V}^{\varepsilon}_{q,p}(\omega,\tau,z=-L)=\delta_0(\tau)\mathbf{1}_0(q)\mathbf{1}_0(p).$$

Applying a diffusion-approximation theorem [3, Section 3.14] establishes that the processes $\tilde{V}^{\varepsilon}_{q,p}$ converge to diffusion processes as $\varepsilon\to 0$. In particular the expectations $\mathbb{E}[\tilde{V}^{\varepsilon}_{p,p}(\omega,\tau,z)]$ converge to $\tilde{v}_p(\omega,\tau,z)$ which obey the closed system of transport equations:

$$\begin{aligned}&\frac{\partial\tilde{v}_p}{\partial z}+2p\frac{\partial\tilde{v}_p}{\partial\tau}=(\tilde{\mathcal{L}}_\omega\tilde{v})_p-2\alpha_m(1-\delta_m)\omega^2(p+\frac{1}{2})^2\tilde{v}_p\\&(\tilde{\mathcal{L}}_\omega\phi)_p=\frac{1}{2}\alpha_n\delta_n\omega^2\left((p+1)^2(\phi_{p+1}-\phi_p)+p^2(\phi_{p-1}-\phi_p)\right)\\&\qquad\qquad-\frac{1}{2}\alpha_n(1-\delta_n)\omega^2((p+1)^2+p^2)\phi_p,\\&\tilde{v}_p(\omega,\tau,z=-L)=\delta_0(\tau)\mathbf{1}_0(p).\end{aligned}\tag{8.1}$$

We then get the limit of the autocorrelation function of the transmission coefficient:

$$\mathbb{E}\left[T^{\varepsilon}_{ii}(\omega+\frac{\varepsilon h}{2},-L,0)\overline{T^{\varepsilon}_{i}}(\omega-\frac{\varepsilon h}{2},-L,0)\right]\overset{\varepsilon\to0}{\longrightarrow}\int\tilde{v}_0(\omega,\tau,0)e^{-ih\tau}d\tau$$

8.2. Convergence of the refocused pulse. Applying the same strategy as in Section 7, we introduce the family of processes $\tilde{W}_p$ that satisfy the system

$$\begin{aligned}&d\tilde{W}_p+2p\frac{\partial\tilde{W}_p}{\partial\tau}dz=2i(\frac{1}{2}+p)\omega\sqrt{\alpha_m(1-\delta_m)}\tilde{W}_p\circ dB_z+\tilde{\mathcal{L}}_\omega\tilde{W}_p dz\\&\tilde{W}_p(\omega,\tau,z=-L)=\delta_0(\tau)\mathbf{1}_0(p)\end{aligned}\tag{8.2}$$

driven by a single Brownian motion B, and we finally get the following result.

THEOREM 8.1. *The refocused signal* $\left(p_{ref(TRT)}(t_1+L+\varepsilon t,z=0)\right)_{t\in(-\infty,\infty)}$ *converges in distribution as* $\varepsilon\to0$ *to*

$$P_{ref(TRT)}(t)=\int\Lambda^{L}_{tr}(\omega,d\tau)\overline{\hat{f}}(\omega)e^{i\omega t}G_{t_0,t_1}(\tau)d\omega$$

where $\Lambda^{L}_{tr}(\omega,d\tau)=\tilde{W}_0(\omega,d\tau,0)$ *is the random measure given by the system (8.2). We can also write that*

$$P_{ref(TRT)}(t)=\left(f(-\,\cdot)*K_{TRT}(\cdot)\right)(t).$$

The Fourier transform of the kernel K_{TRT} is the convolution of the time-inverted cut-off function G_{t_1} with the measure $\tau \mapsto \Lambda_{tr}^L(\omega,\tau)$ evaluated at 0:

$$\hat{K}_{TRT}(\omega) = \left(G_{t_0,t_1}(-\,\cdot) * \Lambda_{tr}^L(\omega,\cdot)\right)(0) = \int G_{t_0,t_1}(\tau)\Lambda_{tr}^L(\omega,d\tau).$$

We can interpret the transport equation in terms of a jump Markov process. Let us introduce the process $(\tilde{X}_t)_{t\geq 0}$ with state space $\mathbb{N}\cup\partial$ and infinitesimal generator $\tilde{\mathcal{L}}$ given by (8.1). When the jump process reaches the state $x\in\mathbb{N}^*$, a random clock with exponential distribution and mean $\tau(\omega,x) = 2\left[\alpha_0\omega^2\left((x+1)^2+x^2\right)\right]^{-1}$ starts running. When the clock strikes, the process is killed and goes to ∂ with probability $p_\partial = 1-\delta_n$, it jumps to $x+1$ with probability $p_{+,x} = \delta_n\frac{(x+1)^2}{(x+1)^2+x^2}$, finally it jumps to $n-1$ with probability $p_{-,x} = \delta_n\frac{x^2}{(x+1)^2+x^2}$. We have

$$\int_{\tau_0}^{\tau_1}\tilde{W}_0(\omega,d\tau,0) = \tilde{\mathbb{E}}_0\Big[\mathbf{1}_{\int_0^L 2\tilde{X}_s ds\in[\tau_0,\tau_1]}\mathbf{1}_{\tilde{X}_L=0} \times\exp\left(2i\omega\sqrt{\alpha_m(1-\delta_m)}\int_0^L(\frac{1}{2}+\tilde{X}_s)dB_s\right)\Big] \tag{8.3}$$

where $\tilde{\mathbb{E}}_{x_0}$ stands for the expectation over the distribution of the jump process starting from $\tilde{X}_0 = x_0$. It should be noted that $\tilde{W}_0$ is not a density with respect the Lebesgue measure over $\mathbb{R}^+$ (while W_1 is a density as seen in Section 7). It consists actually of the sum of a Dirac mass at 0 and a density:

$$\tilde{W}_0(\omega,d\tau,0) = p_{\omega,d}\delta_0(d\tau) + \tilde{W}_{0,c}(\omega,\tau,0)d\tau.$$

This expression is obtained by disintegrating the right-hand side of Eq. (8.3) over the first jump time of the process $(\tilde{X})_{t\geq 0}$. The weight of the Dirac mass is

$$p_{\omega,d} = \exp\left(-\frac{\alpha_n\omega^2 L}{2} + i\omega\sqrt{\alpha_m(1-\delta_m)}B_L\right)$$

This part of the kernel results from the double action of the ODA theory on the front pulse. The pulse spreading is deterministic, but the fluctuations of the medium have changed so that we observe a random time delay which is equal to

$$T_d = \sqrt{\alpha_m(1-\delta_m)}B_L \tag{8.4}$$

The absolutely continuous part is given by

$$\int_0^{\tau_1}\tilde{W}_{0,c}(\omega,\tau,0)d\tau = \int_0^L\frac{\alpha_n\delta_n\omega^2}{2}\exp\left(-\frac{\alpha_n\omega^2(L-t)}{2} + i\omega\sqrt{\alpha_m(1-\delta_m)}B_{L-t}\right) \times\tilde{\mathbb{E}}_1\left[\mathbf{1}_{\int_0^t 2\tilde{X}_s ds\in[0,\tau_1]}\mathbf{1}_{\tilde{X}_t=0}\exp\left(2i\omega\sqrt{\alpha_m(1-\delta_m)}\int_0^t(\frac{1}{2}+\tilde{X}_s)dB_{L-t+s}\right)\right]dt.$$

It does not seem possible to derive a closed form expression for the continuous part. We can either derive expansions, or perform numerical simulations based on Monte-Carlo simulations of the random jump process $(\tilde{X}_t)_{t\geq 0}$.

8.3. Pulse stabilization for a particular class of perturbations. The following theorem expresses the self-averaging property of the refocused pulse in the case $\delta_m = 1$.

THEOREM 8.2. *If $\delta_m = 1$, then the signal $\left(p_{tr(TRT)}(t_1 + L + \varepsilon t, z = 0)\right)_{t\in(-\infty,\infty)}$ converges in probability to $P_{tr(TRT)}(t)$ as $\varepsilon \to 0$ where $P_{tr(TRT)}$ is the deterministic refocused pulse shape:*

$$P_{tr(TRT)}(t) = \left(f(-\,\cdot) * K_{TRT}(\cdot)\right)(t).$$

The Fourier transform of the kernel K_{TRT} is the convolution of the time-inverted cut-off function G_{t_0,t_1} with the measure $\tau \mapsto \Lambda^L_{tr}(\omega,\tau)$ evaluated at 0:

$$\hat{K}_{TRT}(\omega) = \left(G_{t_0,t_1}(-\,\cdot) * \Lambda^L_{tr}(\omega,\cdot)\right)(0) = \int G_{t_0,t_1}(\tau)\Lambda^L_{tr}(\omega, d\tau).$$

8.4. Analysis of the refocused pulse shape. Let us analyze the refocused pulse in the relevant configuration where we record the complete transmitted pulse so that we may assume that $G_{t_0,t_1} \equiv 1$. The kernel K_{TRT} can then be split into two different parts

$$\hat{K}_{TRT}(\omega) = \hat{K}_{TRT,d}(\omega) + \hat{K}_{TRT,c}(\omega)$$

where $\hat{K}_{TRT,d}$ is the contribution of the recorded front pulse

$$\hat{K}_{TRT,d}(\omega) = \exp\left(-\frac{\alpha_n \omega^2 L}{2} + i\omega T_d\right)$$

T_d is the time delay (8.4), and $\hat{K}_{TRT,c}$ is the contribution of the recorded coda

$$\hat{K}_{TRT,c}(\omega) = \int_0^\infty \tilde{W}_{0,c}(\omega,\tau,0)d\tau$$

The recorded front pulse and its contribution to the refocused pulse do not depend on the correlation degree between the media (η_i,ν_i) and (η_{ii},ν_{ii}), up to a simple random time delay. This is expected: The pulse spreading described by the ODA theory is deterministic, it depends only on the statistical distribution of the random fluctuations of the medium, and not on the particular realization. The contribution of the coda is very sensitive to the correlation degree.

We can compute more precisely the expectation of the convolution kernel K_{TRT}. This kernel imposes the mean refocused pulse shape. In the particular framework $\delta_m = 1$, this computation actually yields the deterministic kernel K_{TRT} and the deterministic pulse shape. We find that the expectation of the kernel K_{TRT} is a function of δ_0 and $\alpha_0\omega^2 L$:

$$\mathbb{E}[\hat{K}_{TRT}](\omega) = \mathbb{E}[\hat{K}_{TRT,d}](\omega) + \mathbb{E}[\hat{K}_{TRT,c}](\omega)$$

The contribution of the recorded front pulse is a Gaussian kernel

$$\mathbb{E}[\hat{K}_{TRT,d}](\omega) = \exp\left(-\frac{\alpha_0\omega^2 L}{2}\right)$$

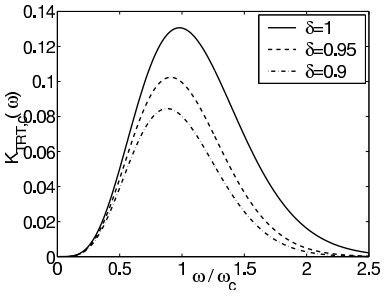

FIG. 8.1. *Mean filter* $\mathbb{E}[\hat{K}_{TRT,c}]$ *as a function of the frequency* ω *for different correlation degrees (total record). Here* $\omega_c = 2/\sqrt{\alpha_0 L}$.

The contribution of the recorded coda $\mathbb{E}[K_{TRT,c}]$ is a medium-band filter. The optimal frequency of the filter is in the constant medium configuration $\delta_0 = 1$:

$$\omega_c|_{\delta_0=1} = \frac{2}{\sqrt{\alpha_0 L}},$$

and the expectation of the kernel $\hat{K}_{TRT,c}$ reads as:

$$\mathbb{E}[\hat{K}_{TRT,c}](\omega)\Big|_{\delta_0=1} = \frac{4}{\sqrt{\pi}} \exp\left(-\frac{\alpha_0\omega^2 L}{8}\right) \int_0^\infty \frac{x^2 e^{-x^2}}{\cosh\left(\sqrt{\alpha_0\omega^2 L/2}x\right)} dx - \exp\left(-\frac{\alpha_0\omega^2 L}{2}\right)$$

As the correlation degree decreases, both the optimal frequency and the gain of the filter decay (see Fig. 8.1). $\mathbb{E}[\hat{K}_{TRT}](\omega)$ is a complicated function of $\alpha_0\omega^2 L$ and δ_0. Introducing the matrix $\tilde{M}_{\delta_0}$:

$$\tilde{M}_{\delta_0} = \begin{pmatrix} -1 & \delta_0 & 0 & \dots & & & \dots & 0 \\ \delta_0 & -5 & 4\delta_0 & 0 & & & & \vdots \\ 0 & 4\delta_0 & -13 & 9\delta_0 & 0 & & & \\ \vdots & \ddots & \ddots & \ddots & \ddots & & & \\ \vdots & & 0 & (j-1)^2\delta_0 & -d(j) & j^2\delta_0 & 0 & \\ 0 & \dots & & \ddots & \ddots & \ddots & \ddots & \ddots \end{pmatrix},$$

where $d(j) = j^2 + (j-1)^2$, the expectation of the kernel $\hat{K}_{TRT}$ is given by

$$\mathbb{E}[\hat{K}_{TRT}](\omega) = \left(\exp(\tilde{M}_{\delta_0}\frac{\alpha_0\omega^2 L}{2})\right)_{11}$$

Figure 8.1 has been obtained by a numerical evaluation of this exponential matrix. It appears that low frequencies are much less attenuated by time perturbations of the medium than high frequencies.

9. Numerical experiments. The acoustic equations are solved by a Lagrangian method along characteristics. The method is very efficient and gives place to

exact radiation conditions at the ends of the computational domain. We briefly describe this method, but details will be presented elsewhere [2]. First the acoustic system (2.1-2.2) is written in the form

$$(\partial_t + \partial_x)A = -r\ B$$
$$(\partial_t - \partial_x)B = r\ A.$$

Note that the characteristics for this system are straight lines. The right and left going modes are

$$A = \zeta^{1/2}u + \zeta^{1/2}p$$
$$B = -\zeta^{1/2}u + \zeta^{1/2}p.$$

The impedance $\zeta = (\rho(x)K(x))^{1/2}$ is written as a function of the travel time $x = \int_0^z ds/c(s)$, where the acoustic sound speed is $c(x) = (K(x)/\rho(x))^{1/2}$. The right and left modes are coupled through the reflectivity $r(x) = 0.5\partial_x\zeta(x)/\zeta(x)$. The advection operators $(\partial_t \pm \partial_x)$ are discretized along characteristics using central differences. The evolution scheme takes the form

$$\vec{v}^{\,(n+1)} = M\vec{v}^{\,(n)}, \qquad \vec{v} = (A, B)^T.$$

In [2] it is shown that M is orthogonal and therefore the scheme is conservative. The Lagrangian scheme is also compared to an operator splitting scheme which leads to similar results.

The mesh is defined in travel time and time. The computational domain is composed by a long random medium with (short) homogeneous extremes. At the ends of the computational domain A and B decouple. This gives rise to exact radiation conditions along the outgoing characteristics. Moreover in the time reversal experiments the (long) time reversed signal can be emitted along the incoming characteristic of the domain without interfering with its corresponding outgoing reflected signal. At the homogeneous ends, x is identical to z (since the background speed is one) and it is very easy to recover the physical variables u and p.

In a first series of experiments we consider a time-independent medium where only the density is randomly varying ($\eta_i = \eta_{ii} = 0$). More precisely the density fluctuations $\nu_i = \nu_{ii}$ are piecewise linear. The nodes are equally spaced with increment $h = 0.02$. The value taken by the process at node jh, $j \in \mathbb{N}$, is denoted by X_j. The $(X_j)_{j\in\mathbb{N}}$ is a sequence of independent and identically distributed (i.i.d.) random variables with a uniform distribution over $[-0.5, 0.5]$. The initial pulse is the derivative of a Gaussian with unit width and amplitude. We use a square cut-off function $G_{t_1}(t) = \mathbf{1}_{[0,t_1]}(t)$ with $t_1 = 100$. Forty different realizations of the process ν have been simulated, and the refocused pulse shapes for each realization are plotted in Fig. 9.1. We get excellent statistical stability of the refocused pulse as predicted by the theory. Furthermore, the refocused pulse shape is in agreement with the theoretical formula (convolution of the initial pulse shape with the kernel (7.18)) as shown by Fig. 9.3a.

The second series of experiments were devoted to time-dependent media. Once again only the density is randomly varying, but now $\nu_i \neq \nu_{ii}$ giving rise to $\delta_m = \delta_n = 0.75$. We can clearly see in Fig. 9.2 that statistical stability has been lost. However the averaged refocused pulse shape is fully predictable by the theoretical formula (convolution of the original pulse shape with the kernel (7.19)) as shown by Fig. 9.3b. By comparing Figs. 9.3a and 9.3b we can check that the averaged refocused pulses

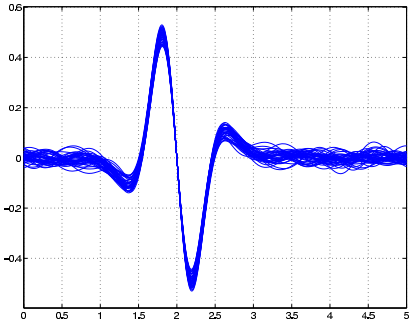

FIG. 9.1. *Refocused pulse shapes. Only the density is random* $\kappa_i = \kappa_{ii} \equiv 1$ *so that* $\alpha_m = \alpha_n$. *The medium is time-independent* $\rho_i = \rho_{ii}$ *so that* $\delta_m = \delta_n = 1$. *We plot* 40 *different numerical experiments performed with different realizations of the medium with the same statistical distribution.*

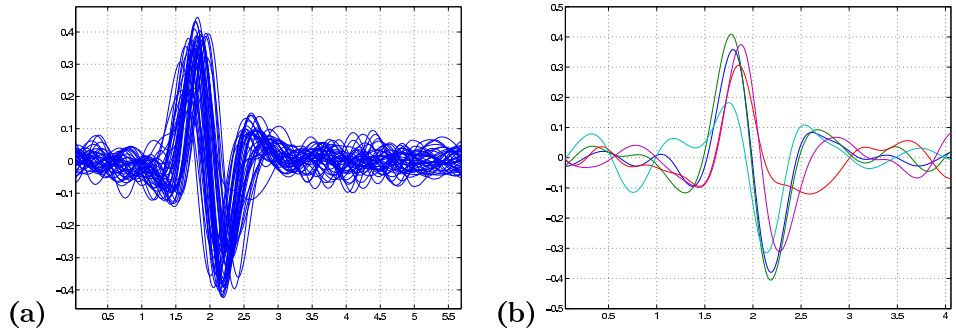

FIG. 9.2. *Refocused pulse shapes. Only the density is random* $\kappa_i = \kappa_{ii} = 1$ *so that* $\alpha_m = \alpha_n$. *Here the fluctuations of the density of the medium is time-varying* $\rho_i \neq \rho_{ii}$ *with* $\delta_m = \delta_n = 0.75$. *The results from* 40 *different numerical experiments are plotted in the left picture.* 5 *individual refocused pulse shapes are taken from this set and plotted in the right picture.*

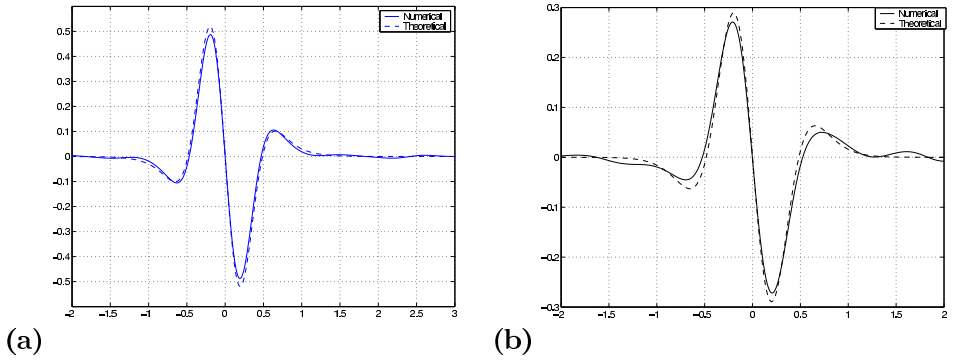

FIG. 9.3. *Comparison of the averaged refocused pulse from the numerical experiments and the mean refocused pulse shape obtained by the asymptotic theory. Picture a: without time perturbation* $\delta_m = \delta_n = 1$ *(corresponding to Fig. 9.1. Picture b: with time perturbation* $\delta_m = \delta_n = 0.75$ *(corresponding to Fig. 9.2).*

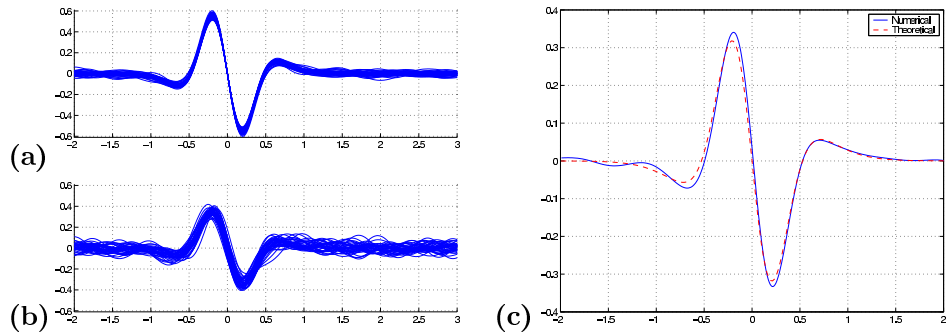

FIG. 9.4. *Refocused pulse shapes for a Goupillaud medium with* $\delta_m = 1$. *Both the density and the compressibility are random. Picture a: refocused pulse shapes for* 40 *different realizations without time perturbation* $\delta_n = 1$. *Picture b: the same with time perturbation* $\delta_n = 0.7$. *Picture c: comparison between the theoretical expected pulse shape and the numerically averaged pulse shape for the case* $\delta_n = 0.7$.

for the time-independent and the time dependent cases are very similar in shape up to an amplitude reduction factor of order 2.

We now consider a Goupillaud medium which is widely used in the literature [3, 5] and which enables the exact calculations of the reflection and transmission coefficients. In this particular case $\rho(x)$ and $K(x)$ are piecewise constant with jump discontinuities along each layer's interface. These coefficients are such that the travel time across each layer is the same. Accordingly the transmission-reflection matrix $\tilde{M}$ is known exactly and there is no need to discretize the partial differential equation given above [5] since we get directly

$$\vec{v}^{\,(n+1)} = \tilde{M}\vec{v}^{\,(n)}, \qquad \vec{v} = (A, B)^T.$$

We have performed a series of experiments with a Goupillaud medium where the travel time across each layer is $h = 0.01$. The values of the density and bulk modulus fluctuations ν and η inside each layer are a sequence of i.i.d. random variables, giving rise to a sequence of random impedances. We compare the results from time reversal experiments in absence and in presence of time-fluctuations of the medium. Note that the travel times are not affected by the time-perturbation so that $\delta_m = 1$. This means that time-dependent Goupillaud media belong to the class of media which exhibit statistical stability with respect to time fluctuations. These theoretical predictions are confirmed by the numerical simulations presented in Fig. 9.4. We can observe the enhanced statistical stability even in presence of strong time fluctuations $\delta_n = 0.7$ (compare with Fig. 9.2). Again the numerically averaged refocused pulse shape is in very good agreement with the expected refocused profile.

10. Conclusion. We have analyzed the impact of time fluctuations of a random medium on the pulse refocusing during a time-reversal experiment. We have demonstrated that a coherent refocused pulse can still be observed even in the presence of moderate time-perturbations. The recompression of the incoherent reflected signal is very robust in the sense that we always observe a refocused pulse as soon as some correlation degree persists between the two snapshots of the medium. However statistical stability of refocusing is lost in that the refocused pulse shape usually depends on the realizations of the snapshots. Special media such as Goupillaud-type media preserve a strong degree of stabilization, while more general media do not.

Acknowledgements. This work was supported by the ONR grant N00014-02-1-0089. J. Garnier also acknowledges support from the program ACI-NIM-2003-94. A. Nachbin and D. G. Alfaro Vigo were supported by CNPq/Brazil under grant 300368/96-8.

REFERENCES

[1] M. Abramowitz and I. Stegun, *Handbook of mathematical functions* (Dover, New York, 1965).
[2] D. G. Alfaro Vigo, A. G. Silva Correia, and A. Nachbin, Complete time-reversed refocusing in reflection with an acoustic Lagrangian model, in preparation.
[3] M. Asch, W. Kohler, G. Papanicolaou, M. Postel, and B. White, Frequency content of randomly scattered signals, SIAM Rev. **33** (1991) 519-625.
[4] G. Bal, G. Papanicolaou, and L. Ryzhik, Self-averaging in time reversal for the parabolic wave equation, Stochastics and Dynamics **2** (2002) 507-531.
[5] L. Berlyand and R. Burridge, The accuracy of the O'Doherty-Anstey approximation for wave propagating in highly disordered stratified media, Wave Motion **21** (1995) 357-373.
[6] P. Blomgren, G. Papanicolaou, and H. Zhao, Super-resolution in time-reversal acoustics, J. Acoust. Soc. Am. **111** (2002) 230-248.
[7] R. Burridge, G. Papanicolaou, and B. White, Statistics for pulse reflection from a randomly layered medium, SIAM J. Appl. Math. **47** (1987) 146-168.
[8] J.-F. Clouet and J.-P. Fouque, Spreading of a pulse traveling in random media, Annals of Applied Probability **4** (1994) 1083-1097.
[9] J.-F. Clouet and J.-P. Fouque, A time-reversal method for an acoustical pulse propagating in randomly layered media, Wave Motion **25** (1997) 361-368.
[10] A. Derode, A. Tourin, J. de Rosny, M. Tanter, S. Yon, and M. Fink, Taking advantage of multiple scattering to communicate with time reversal antennas, Phys. Rev. Lett. **90** (2003) 014301.
[11] M. Fink, Time reversed acoustics, Scientific American (November 1999) 91-97.
[12] M. Fink, G. Montaldo, and M. Tanter, Time reversal acoustics in biomedical engineering, Annual Review of Biomedical Engineering **5** (2003) 465-497.
[13] J.-P. Fouque and K. Sølna, Time-reversal aperture enhancement, SIAM Multiscale Modeling and Simulation **1** (2003) 239-259.
[14] H. J. Kushner, *Approximation and weak convergence methods for random processes* (MIT Press, Cambridge, 1984).
[15] P. Lewicki, R. Burridge, and G. Papanicolaou, Pulse stabilization in a strongly heterogeneous medium, Wave Motion **20** (1994) 177-195.
[16] R. F. O'Doherty and N. A. Anstey, Reflections on amplitudes, Geophysical Prospecting **19** (1971) 430-458.
[17] G. Papanicolaou, Wave propagation in a one-dimensional random medium, SIAM J. Appl. Math. **21** (1971) 13-18.
[18] G. Papanicolaou, Asymptotic analysis of stochastic equations, in MAA Stud. in Math. **18**, M. Rosenblatt, ed., Mathematical Association of America, 1978, pp. 111-179.
[19] G. Papanicolaou, L. Ryzhik and K. Sølna, Statistical stability in time reversal, to appear in SIAM J. Appl. Math. (2003).
[20] C. Prada, E. Kerbrat, D. Cassereau, and M. Fink, Time reversal techniques in ultrasonic nondestructive testing of scattering media, Inverse Problems **18** (2002) 1761-1773.
[21] K. Sølna, Focusing of time-reversed reflections, Waves in Random Media **12** (2003) 365-385.
[22] K. Sølna and G. Papanicolaou, Ray theory for a locally layered medium, Waves in Random Media **10** (2000) 151-198.
[23] A. Tourin, A. Derode, and M. Fink, Sensitivity to perturbations of a time-reversed acoustic wave in a multiple scattering medium, Phys. Rev. Lett. **87** (2001) 274301.